JOURNAL OF CHEMICAL & ENGINEERING DATA

ARTICLE

pubs.acs.org/jced

Density Measurements of Endothermic Hydrocarbon Fuel at Sub- and Supercritical Conditions

H. W. Deng,[†] C. B. Zhang,[*,†] G. Q. Xu,[†] Z. Tao,[†] B. Zhang,[†] and G. Z. Liu[‡]

[†]National Key Laboratory of Science and Technology on Aero-Engine Aero-thermodynamics, School of Jet Propulsion, Beijing University of Aeronautics and Astronautics, Beijing, 100191, P. R. China

[‡]School of Chemical Engineering and Technology, Tianjin University, Tianjin, 300072, P. R. China

ABSTRACT: The density of a typical endothermic hydrocarbon fuel (RP-3) at sub- and supercritical conditions is measured using a novel density measurement method which is based on mass conservation equation and can be applied to the density measurement of single phase flow including supercritical fluids. The measurement covers the temperature range of (295 to 796) K under pressures from (0.1 to 5) MPa. The uncertainty of the measurement is within ± 0.635 % according to error analysis. The results are fitted as polynomials to analyze deviations. For the 265 experimental data points, the average absolute deviation (AAD) and the maximum absolute deviation (MAD) are 0.539 % and 3.29 %, respectively. In addition, the isobaric thermal expansion α_P is derived from the fitted values of density.

1. INTRODUCTION

Future aircrafts will fly faster, have more heat generating electronics, and operate with higher engine pressure and fuel/air ratios compared to today's aircrafts, all of which will increase the heat load to the aircraft materials. Efficient cooling technology is one of the critical methods to reduce the thermal stress and heat load. Fuel-cooled aircraft thermal management systems are popularly used with a minimum weight penalty and technical risk.[1] The Versatile Affordable Advanced Turbine Engines (VAATE) and Integrated High Performance Turbine Engine Technology (IHPTET) program show that more and more cooling requirements are needed, and then the fuel temperature is through and beyond the critical region under the limitation of fuel supply. To minimize the carried fuel volume of aircrafts, high densities of endothermic hydrocarbon fuels are needed. The thermophysics properties of fuel are required to be well-known for the safety of application. The database of properties for the fuel such as vapor pressure, specific heat, density, viscosity, surface tension, and critical parameters is necessary to predict the performance of components and to shorten the design cycle of engine.[2] Systematic studies of those thermophysics properties of mixtures and their excess properties as functions of temperature and concentration can give insight into the molecular structure of mixtures and provide information on the interaction between components, which are essential for designing and testing theoretical models of mixtures.[3]

Density is an important property required in a wide range of engineering disciplines as well as in the determination of different fluid properties. The densities of pure compounds[4−8] and binary mixtures[2,3,9−12] have been investigated by lots of researchers using a vibrating tube densimeter. Although the vibrating tube densimeter is one of the most popular methods for density measurement, it is only suitable for low temperature density measurements, and its accuracy is affected by the viscosity of fluids.

In this work, we present a novel density measurement of homogeneous phase fluid based on the mass conservation equation. Using this method, the densities of a typical endothermic hydrocarbon fuel (RP-3) at sub- and supercritical conditions are measured. The paper is organized as follows: in Section 2, we describe the experimental apparatus and procedures; in Section 3, we verify the validity of the method and measured the density of hydrocarbon fuel under sub- and supercritical conditions. In Section 4, we end this study with concluding remarks in view of the results section.

2. EXPERIMENTAL SECTION

2.1. Materials. A typical jet fuel RP-3 is used in this work. Composition analysis by using GC6890-MS5975 shows that RP-3 consists of 52.44 % alkanes, 7.64 % alkenes, 18.53 % benzenes, 15.54 % cycloalkanes, 4.39 % naphthalenes, and 1.46 % other; the detailed compositions of RP-3 are listed in Table 1. The critical point of RP-3 was identified as (T_c = 645.04 K, P_c = 2.34 MPa) due to the most obvious critical opalescence phenomenon in our previous work. Besides, the phase transient point of RP-3 at 2 MPa was determined as 601.3 K. Water used in this work is double-distilled.

2.2. Facility. Figure 1 shows the experimental system. It includes a preparative system, measured system, and reclaimed system.

In the preparative system, the fuel in tank 1 is pumped up to 12 MPa by a piston pump (2J-Z 104/16). A 45 μm filter (filter 1 of Figure 1) is attached to the suction side of the piston pump both to protect the pump from any entrained debris and to serve as an inlet accumulator to ensure the pump is not starved on the suction stroke. The prepressed fuel from the piston pump is pushed

Received: April 3, 2011
Accepted: May 12, 2011
Published: May 20, 2011

ACS Publications © 2011 American Chemical Society

dx.doi.org/10.1021/je200258g | J. Chem. Eng. Data 2011, 56, 2980–2986

Table 1. Detailed Analysis of Fuel Composition for RP-3 Jet Fuel

no.	composition	mass fraction
1	*n*-hexane	0.0037
2	*n*-octane	0.0076
3	*n*-nonane	0.0252
4	*n*-decane	0.0578
5	*n*-undecane	0.0439
6	*n*-dodecane	0.0384
7	*n*-tridecane	0.0321
8	*n*-tetradecane	0.0165
9	*n*-pentadecane	0.0057
10	*n*-hexadecane	0.0059
11	*n*-heptadecane	0.0308
12	2-methyloctane	0.0108
13	3-methyloctane	0.0153
14	4-methyloctane	0.0172
15	2-methylnonane	0.0093
16	3-methylnonane	0.0105
17	4-methylnonane	0.0128
18	2-methyldecane	0.0145
19	3-methyldecane	0.0155
20	4-methyldecane	0.0178
21	5-methyldecane	0.0194
22	2-methylundecane	0.0148
23	3-methylundecane	0.0166
24	4-methylundecane	0.0170
25	5-methylundecane	0.0225
26	2-methyldodecane	0.0076
27	3-methyldodecane	0.0093
28	4-methyldodecane	0.0128
29	5-methyldodecane	0.0133
30	6-dimethyl-2-octene	0.0187
31	4-propyl-3-heptene	0.0318
32	2-methylpentalene	0.0259
33	1,2,3-trimethyl benzene	0.0448
34	1,3,5-trimethyl benzene	0.0327
35	1-ethyl-3-methyl benzene	0.0781
36	2-ethenyl-1,3-dimethyl benzene	0.0298
37	cyclododecane	0.0117
38	1-hexylcyclopentane	0.0420
39	1-butyl-2-ethyl cyclopentane	0.0134
40	1,1,3-trimethyl cyclohexane	0.0211
41	1-butylcyclohexane	0.0428
42	1-heptylcyclohexane	0.0056
43	1-ethyl-4-methylcyclohexane	0.0187
44	1-methyl-naphthalene	0.0245
45	2-methyl-naphthalene	0.0194
46	other	0.0146

into an attached airbag pulsation damper (NXQ-L04/16-H) to reduce the pressure pulsation to lower than 0.5 % of the test section inlet pressure. The fuel from the damper is divided into a major path fuel and a bypass fuel: the latter was collected for reuse, and its pressure was controlled by a back pressure valve (0 to 15) MPa in the bypass system; the mass flow rate of the major path fuel is measured using a Coriolis-force flow meter (DMF-1-1, 0.15 %), and a 30 μm filter is installed to the upstream of the flow control valve (SS-426F3) to protect the fine passages in it. To achieve the required inlet fuel temperature of the test section, the prepressurized major path fuel is heated (up to 830 K) by two preheaters (Preheater 1 and Preheater 2) which are controlled by independent available current power supplies with a capacity of 20 kW.

In the test section, a pressure gauge transducer (model 3051CA4, Rosemount) is used to measure the static pressure at the inlet of the test section. The fuel temperature is measured at the inlet and outlet of the test tube with K-type armored thermocouples, respectively. All data are recorded using the computer system.

After testing, the hot fuel is cooled lower than 310 K by a water cooled shell and tube heat exchanger, and then the fuel pressure releases to ambient pressure through a back pressure valve. The fuel is collected into tank 2 for other usages, and the water out from the heat exchanger is cooled in cooling tower and then collected into tank 3 for recycling.

2.3. Test Section. The detailed configuration of the test section is shown in Figure 2: the inside and outside diameters and the length of the test tube (no. 4 in Figure 2) are 7 mm, 10 mm, and 510 mm, respectively. The test tube is mounted vertically within a vacuum chamber ($\leq$ 53 Pa) to minimize convection and thermal conduction. The wall of the test tube is covered using high reflective metal (1Cr-18Ni-9Ti) with a thickness of 0.2 mm to minimize the heat loss due to radiation in the vacuum environment. At the inlet and outlet of the test tube B and C, flow mixers are installed to mix the fluid and ensure homogeneous temperature. The fuel temperature is measured by armored K-type thermocouple, and the diameter of the armor is 1.0 mm. The electronic signal is captured by the Intelligent Device Debugging Assistant (IDDA, a data acquisition software) of Beihang University with the frequency of 150 Hz. The density measurement apparatus has been applied as a patent (No. CN101936865A).

2.4. Principle and Error Analysis. The density measurement is based on the mass conservation equation, as follows:

$$\dot{m} = \rho U A \tag{1}$$

where $\dot{m}$, ρ, U, and A represent the mass flow rate, density, velocity, and section area, respectively.

The velocity is determined by the length (L) of test tube and the resident time (Δt) of the fluid in a test tube for single phase flow, and it is defined as

$$U = \frac{L}{\Delta t} \tag{2}$$

where the resident time Δt is identified by the response of thermocouples to the temperature changes at the inlet and outlet of the test tube as follows: in experiments, the temperature of the upstream of the test tube rises suddenly, and then, the response time of inlet thermocouple is recorded as t_1, while the response time of outlet thermocouple is t_2, the resident time $\Delta t = t_2 - t_1$. The section area A is defined as

$$A = \pi \frac{d^2}{4} \tag{3}$$

where d is the inside diameter of the test tube. According to eqs 1 to 3, the density of the fluid can be calculated using

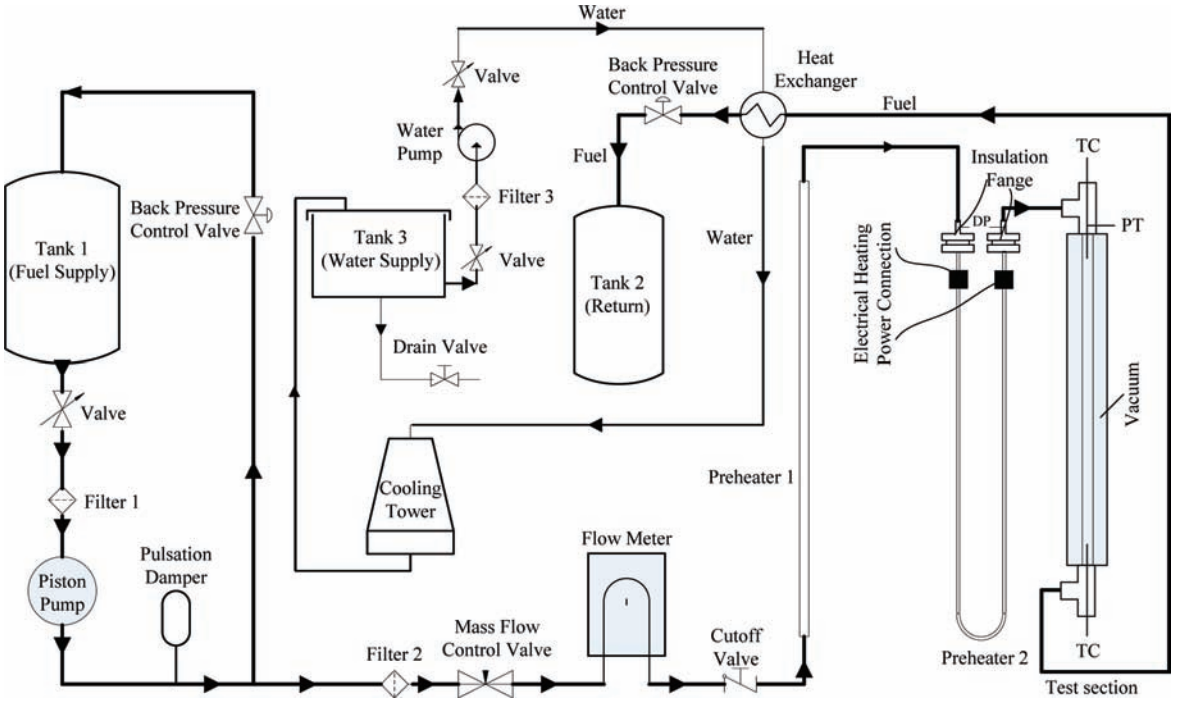

Figure 1. Schematic of the experimental system.

the following equation

$$\rho = 4\frac{\dot{m}\Delta t}{\pi d^2 L} \tag{4}$$

Equation 4 indicates that the accuracy of density measurement is dependent on the measurement accuracies of the mass flow rate $\dot{m}$, the resident time Δt, the inside diameter d, and the length L of the test tube.

In this work, calibration of the mass flow meter through the data acquisition system is accomplished by weighing several flows over timed intervals at a constant upstream pressure and flow rate through a metering valve, and the accuracy is ± 0.15 % of the reading value. The accuracy of length and inside diameter is ± 0.01 mm. Hence, the accuracy of density measurement is mainly determined by the accuracy of resident time measurements.

To minimize the error of Δt, four techniques are applied: (1) The fluid temperature at the inlet and outlet of the test tube should be homogeneous. This condition is carried out by the flow mixers at the inlet and outlet of test tube. (2) Sampling frequency should be quick enough: the higher frequency, the higher accuracy of resident time measurements. In this work, the sampling frequency is 150 Hz, which ensures that the error of resident time measurement is within 3.5 ms. (3) The thermocouples in both the inlet and the outlet should have the same response time; before using, the response time of thermocouples is calibrated by measuring water temperature. (4) The Reynolds number Re should be beyond 3000, and the fluid should flow downward to reduce the convection. But Re is limited by sampling frequency because the measurement error of Δt increases with the increase of Re. On the basis of the sampling frequency in this study, the Reynolds number is between 3500 and 12 000.

In addition, the pressure gauge transducer is calibrated with the pressure calibrator (Mensor PCS400M), and the maximum uncertainty is ± 0.065 % of the full range of 10 MPa corresponding to ± 0.0065 MPa. All of the thermocouples are calibrated in a constant temperature bath, and the measurement accuracy is ± 0.5 K. The minimum resolution of the data acquisition software IDDA is 0.0025 mV, corresponding to 0.06 K of temperature variation which can be used to evaluate the accuracies of time and temperature measurements. According to the formulation of temperature and time:

$$\frac{T - T_0}{T_f - T_0} = 1 - e^{-\tau/\tau_c} \tag{5}$$

where T_0, T_f, and T are the initial, the real, and the transient temperatures of the fluid; τ_c is the time constant of the armored K-type thermocouple, and τ represents measuring time.

In this work, τ_c is about 0.15 s for RP-3 and 0.3 s for water when the fluid temperature is lower than its critical point; about 0.25 s for RP-3 at the critical point and about 0.03 s for RP-3 when its temperature is greater than its critical point. The temperature difference $(T_f - T_0)$ is about 10 K. If the transient temperature difference $(T - T_0)$ is equal to 0.06 K, the corresponding maximum response time of thermocouple is 1.8 ms, which is less than the error of resident time measurement (3.5 ms). In experiments, Δt is greater than 1.5 s, so the relative error of Δt is within ± 0.233 %.

The standard uncertainties of $\dot{m}$, Δt, d, L, and P have been calculated taking into account the expanded uncertainty and the coverage factor $k = 2$. For the calculation of the relative expanded uncertainty of the density measurement, the combined standard uncertainty of density measurement is first calculated as ± 0.635 %, and then the relative expanded uncertainty of density measurement is identified as ± 1.27 %.

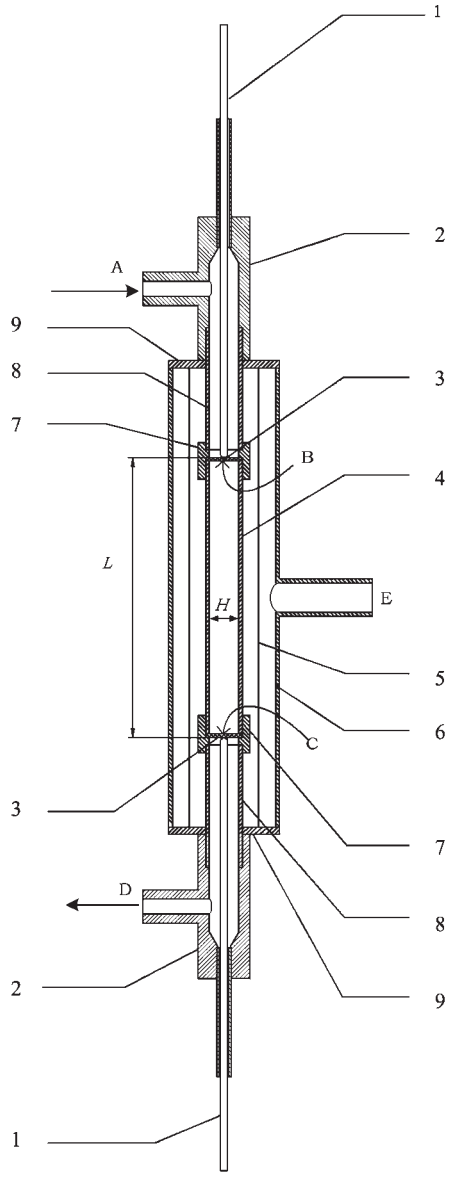

1. thermocouple 2. three-way 3. flow mixer 4. test tube
5. high reflective metal cover 6. vacuum chamber
7. converting tube 8. stable tube 9. cover

Figure 2. Schematic of the test section.

3. RESULTS AND DISCUSSION

3.1. Accuracy and Repeatability. The validity of the method mentioned in this paper is verified by measuring the density of water in the temperature range of (288 to 360) K at ambient pressure (0.1 MPa) and compared with the published data which has an uncertainty of 0.003 %.[13] The measured and published densities of water at ambient pressure (0.1 MPa) are listed in Table 3, where ξ_r is the relative error of density and subscripts "exp", "fit", and "pub" represent experimental, fitted, and the published data, respectively. It is seen from Table 2 that the maximum deviation of density measurement is about −0.9 %; after being fitted, the maximum deviation approaches to −0.8 %.

Table 3 shows three different measurement results of the density of RP-3 at the ambient pressure, and the temperature changes from (295 to 383) K. The density of the second column

Table 2. Relative Error ($\xi_{r,exp}$, $\xi_{r,fit}$) of the Experimental Density (ρ_{exp}) and the Fitted Value (ρ_{fit}) of Water Compared with Published Data ρ_{pub} at 0.1 MPa

T	ρ_{pub}	ρ_{exp}	ρ_{fit}		
K	kg·m^{-3}	kg·m^{-3}	kg·m^{-3}	$\xi_{r,exp}$	$\xi_{r,fit}$
288.59	994.886	988.338	989.130	−0.0066	−0.0058
308.59	991.837	988.334	985.026	−0.0035	−0.0069
314.02	990.187	982.808	983.231	−0.0075	−0.0070
321.70	987.372	978.618	980.279	−0.0089	−0.0072
328.13	984.620	975.768	977.467	−0.0090	−0.0073
336.85	980.402	974.182	973.214	−0.0063	−0.0073
347.91	974.317	967.132	967.188	−0.0074	−0.0073
355.88	969.490	962.913	962.468	−0.0068	−0.0072
359.80	967.457	959.951	960.041	−0.0078	−0.0077

in Table 2 is measured based on the definition of density:

$$\rho = \frac{M}{V} \tag{6}$$

where M and V represent the weight and the volume of the fluids, respectively. They are measured by a precision balance (Sartorius BT 224S, accuracy: 0.1 mg) and precision measuring cylinder (accuracy: 0.1 mL). Then, the uncertainty of this measurement is identified as ± 0.125 %.

In Table 3, the second column is considered as the accurate value; the third one is measured using eq 4, and the fourth is the fitted value of the third column. The fifth and the sixth column are the relative error of ρ_{exp} and ρ_{fit} compared with ρ_{real}, respectively. It can be seen that the maximum relative error in the first and second measurement results are −1.137 % and −1.031 %, respectively. After being fitted, they decrease to −0.894 % and −0.827 %. When the two measurement results are fitted using polynomials, the maximum relative error farther decreases to −0.844 %.

In this paper, all of the experimental density values of RP-3 at a fixed pressure are fitted according to as the following type of polynomials:

$$\rho = \sum_{i=1}^{n} A_i (T/\mathrm{K} - 273.15)^{i-1} \tag{7}$$

where A_i is the temperature polynomial coefficient; n is the number of the polynomial coefficients which is determined by using an F-test.

The results of Tables 2 and 3 show that nearly the same negative deviation accompanies with experiments at different temperatures whether the fluid is water or fuel. It is believed that the deviation is mainly caused by system error especially the heat conduction of fuel and hysteresis of thermocouple response. Thus, a constant coefficient C is used to modify eq 4:

$$\rho = 4\frac{C\dot{m}\Delta t}{\pi d^2 L} \tag{8}$$

where the constant C = 1.001727; it is calculated according the average coefficient of each measured point in Table 2. The experimental density value (ρ_{exp}) is first obtained by eq 4 which is shown in Table 3 and then corrected by eq 8 and compared with the value (ρ_{real}) that obtained by eq 6; the accuracy of the density measurements for RP-3 by eq 8 can be promoted to ± 0.5 %.

dx.doi.org/10.1021/je200258g |J. Chem. Eng. Data 2011, 56, 2980–2986

Table 3. Relative Error ($\xi_{r,exp}$, $\xi_{r,fit}$) of the Experimental Density (ρ_{exp}) and the Fitted Value (ρ_{fit}) of RP-3 Compared with the Accurate Density ρ_{real} at Ambient Pressure

T	ρ_{real}	ρ_{exp}	ρ_{fit}		
K	kg·m^{-3}	kg·m^{-3}	kg·m^{-3}	$\xi_{r,exp}$	$\xi_{r,fit}$
First Measurement Results					
295.71	778.002	771.301	772.787	−0.0086	−0.0067
310.14	767.103	765.180	762.139	−0.0025	−0.0065
320.05	759.816	758.104	754.825	−0.0023	−0.0066
325.67	755.744	749.233	750.675	−0.0086	−0.0067
332.29	751.000	743.608	745.784	−0.0098	−0.0069
343.42	743.157	736.381	737.572	−0.0091	−0.0075
351.74	737.383	729.001	731.429	−0.0114	−0.0081
361.51	730.699	725.451	724.213	−0.0072	−0.0089
362.24	730.204	723.316	723.675	−0.0094	−0.0089
383.97	715.706	709.157	710.634	−0.0092	−0.0071
Second Measurement Results					
304.98	770.962	768.419	764.586	−0.0033	−0.0083
315.69	763.002	757.545	757.699	−0.0072	−0.0070
324.35	756.696	748.897	752.134	−0.0103	−0.0060
336.97	747.679	741.903	744.018	−0.0077	−0.0049
347.43	740.364	735.891	737.300	−0.0060	−0.0041
356.61	734.041	728.830	731.400	−0.0071	−0.0036
368.03	726.294	731.846	724.055	0.0076	−0.0031
372.29	723.443	721.312	721.320	−0.0030	−0.0029
380.16	718.213	716.028	716.259	−0.0030	−0.0027
383.27	716.162	712.358	714.258	−0.0053	−0.0027

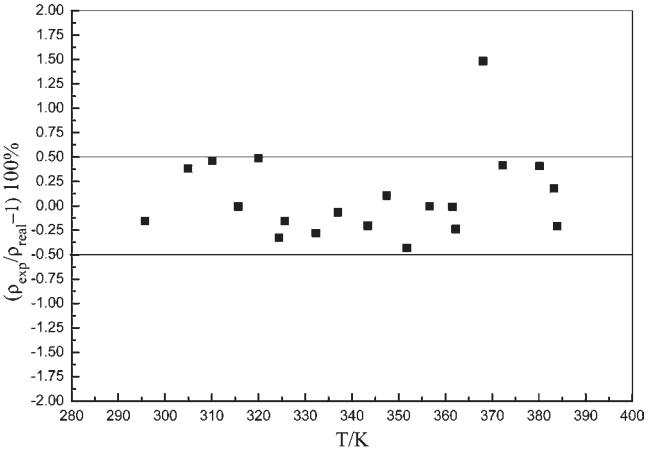

Figure 3. Deviation of $(\rho_{exp}/\rho_{real} - 1)$ versus temperature.

Figure 3 shows the deviation of $(\rho_{exp}/\rho_{real} - 1)$ versus temperature. Out of the 20 data points, 19 data points are within the ± 0.5 % error bound, which is 95 %. The point which is not in the error boundaries may be a gross error in the experiments and is eliminated. For RP-3, the average absolute deviation (AAD = $(1/n)\Sigma_{i=1}^{n}|((\rho_{exp,i}/\rho_{real,i}) - 1)|$) and the maximum absolute deviation (MAD = $|((\rho_{exp,i}/\rho_{real,i}) - 1)|$) are found to be 0.2375 % and 0.4858 %, respectively. After being fitted, AAD = 0.111 % and MAD = 0.1569 %, respectively. The results indicate

Table 4. Fitted Experimental Density (ρ) of RP-3 from T = (295 to 796) K under Sub- and Supercritical Pressures (P = (2 to 5) MPa)

T	ρ	T	ρ	T	ρ	T	ρ
K	kg·m^{-3}	K	kg·m^{-3}	K	kg·m^{-3}	K	kg·m^{-3}
P = 2 MPa							
310.38	770.066	435.89	642.676	567.83	484.398	657.35	94.612
318.49	762.559	437.91	641.138	576.24	474.209	668.81	88.305
336.67	744.377	452.43	621.809	578.74	471.197	669.49	87.944
359.92	723.334	475.25	598.875	589.07	454.794	683.45	80.807
369.81	710.892	486.49	584.637	604.45	428.517	694.63	75.475
378.92	702.955	498.72	569.170	613.13	404.986	705.37	70.646
388.93	692.677	506.80	558.987	624.50	366.761	726.10	62.071
400.26	681.537	521.02	542.147	626.91	354.923	762.03	49.141
409.64	671.511	531.77	528.734	633.14	322.258	780.02	43.379
414.10	666.435	539.98	518.554	637.43	106.575	791.03	40.028
420.54	658.862	554.29	500.916	648.20	99.942		
P = 2.34 MPa							
295.63	788.773	451.17	633.195	611.31	430.746	668.66	104.639
310.38	775.262	461.19	622.037	616.18	422.596	671.40	102.392
318.49	767.733	472.49	609.271	621.94	401.709	698.46	84.824
327.59	759.198	496.67	581.263	626.69	379.390	710.74	78.855
336.67	750.597	522.40	550.377	629.87	361.541	722.58	73.929
345.90	741.753	543.58	524.074	632.35	345.846	732.65	70.247
359.92	728.132	548.95	517.279	633.60	337.315	741.59	67.313
369.81	718.380	563.02	499.208	637.67	306.528	754.03	63.663
378.92	709.287	577.51	480.205	640.28	284.205	757.04	62.847
388.93	699.172	579.83	477.122	641.27	234.193	765.85	60.591
414.19	673.052	595.30	456.305	652.62	120.280	786.82	55.907
435.70	650.110	603.40	445.223	658.71	113.777		
444.32	640.726	609.65	434.420	660.52	111.987		
P = 3 MPa							
295.63	790.774	440.34	648.150	614.50	434.269	677.33	172.485
310.38	777.483	453.57	634.725	626.06	416.681	677.62	171.282
318.49	769.692	459.24	628.948	643.91	372.074	677.79	170.559
327.59	760.362	470.44	617.405	647.77	355.405	685.05	153.592
336.67	750.499	471.84	615.952	650.71	340.348	693.90	127.475
359.92	731.310	501.09	584.282	655.35	312.970	701.55	110.045
369.81	721.733	515.03	568.054	658.14	294.811	713.25	90.710
378.92	711.974	532.79	545.948	658.61	291.635	719.18	83.636
388.93	701.301	542.35	533.293	662.17	267.105	731.35	73.351
393.15	696.826	549.15	523.954	665.24	245.603	729.59	74.549
402.15	687.357	561.85	510.756	666.59	236.185	750.67	64.589
404.78	684.606	567.09	503.966	667.23	231.824	776.70	58.762
408.39	680.855	575.22	492.560	668.68	221.964	794.06	55.736
420.63	668.224	587.50	475.126	670.13	212.448		
433.56	655.028	600.45	455.899	669.88	214.062		
P = 4 MPa							
296.82	791.179	442.71	658.195	581.05	505.954	699.90	177.058
310.37	778.903	450.86	650.790	590.28	497.712	700.14	181.521
319.46	770.902	455.15	646.287	591.33	496.116	704.57	159.131
327.16	764.896	464.64	639.156	603.26	477.350	708.79	142.774
336.53	754.492	469.15	634.252	617.31	454.115	721.75	109.706
346.11	745.782	484.17	617.467	632.39	427.251	729.99	96.365

dx.doi.org/10.1021/je200258g |J. Chem. Eng. Data 2011, 56, 2980–2986

Table 4. Continued

T	ρ	T	ρ	T	ρ	T	ρ
K	kg·m^{-3}	K	kg·m^{-3}	K	kg·m^{-3}	K	kg·m^{-3}
356.09	737.599	493.03	607.241	641.51	409.340	737.26	87.429
370.06	725.864	505.28	592.682	651.92	382.436	745.66	79.346
375.69	721.032	513.70	582.400	658.29	363.673	752.19	74.272
386.39	711.670	524.93	568.288	663.67	349.017	766.36	65.809
392.88	705.884	531.58	559.735	667.87	336.609	784.62	58.294
403.10	696.579	542.82	548.908	686.66	259.145	791.15	56.241
412.75	687.587	552.73	536.454	687.44	255.666		
422.83	677.949	564.13	524.526	688.37	251.426		
432.67	668.301	576.27	513.003	696.19	212.594		
			P = 5 MPa				
295.07	796.458	451.19	659.014	561.62	549.093	694.24	338.691
319.73	775.639	456.73	653.809	570.34	539.779	695.20	334.865
328.67	768.032	467.61	643.501	572.35	537.618	704.09	294.998
339.87	758.456	477.22	634.311	580.74	528.531	711.48	244.650
345.07	753.983	487.04	624.814	596.11	511.627	713.77	231.850
360.28	740.837	498.05	614.045	606.66	499.830	718.46	208.452
372.66	730.028	502.46	609.695	611.85	493.953	727.40	172.380
385.33	718.882	513.11	599.099	634.76	460.539	752.15	111.205
389.96	714.778	521.62	590.533	637.45	456.387	753.79	108.512
425.16	683.088	532.72	579.238	644.25	448.205	796.97	69.789
433.65	675.303	545.02	566.538	649.84	440.550		
442.27	667.332	555.26	555.819	673.90	396.029		

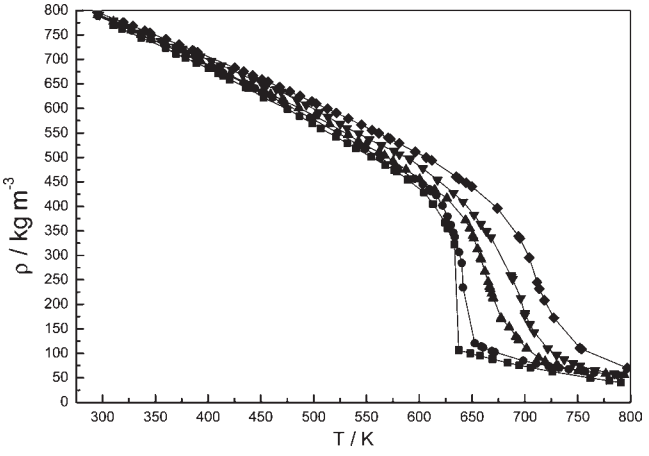

Figure 4. Density variations of RP-3 versus temperature under different pressures. ■, 2 MPa; ●, 2.24 MPa; ▲, 3 MPa; ▼, 4 MPa; ♦, 5 MPa.

that the correction method (eq 8) is feasible, but it should be noted that the uncertainty of density measurement may be greater than ± 0.5 % when the fluid is near phase transient point and critical point due to density fluctuations. In the following part, the density data of RP-3 at sub- and supercritical pressure conditions will be reported, and the effect of temperature and pressure on density will be discussed.

3.2. Density of RP-3. The density of RP-3 has been measured at the temperature range of (295 to 796) K and at pressures from (0.1 to 5) MPa. The densities of which at ambient pressure have been shown in Table 3, continued, the densities of which at sub- and supercritical conditions are listed in Table 4. The pressure and temperature range from (2 to 5) MPa and (295 to 796) K, respectively. The temperature in Table 4 refers to the experimental value, and the density is first corrected by eq 8 and then fitted by polynomials as eq 7. Hence, the critical density of RP-3 has been identified as 221.18 kg·m^{-3}.

Although the accuracy of density measurement has been determined as ± 0.5 % by the density measurement of RP-3 in the temperature range of (295 to 383) K under ambient pressure, the measurement error may increase due to the following factors: (1) small scale bubbles are generated at subcritical pressure; (2) large density fluctuation occurs at the critical point; (3) heat conduction enhances and heat loss increases at higher temperature. Before the critical point, the AAD and the MAD between the measured and fitted values are 0.264 % and 1.52 %, respectively; near the critical point, AAD = 1.05 % and MAD = 2.42 %, respectively; beyond the critical point, AAD = 0.833 % and MAD = 3.29 %, respectively; for all values, AAD = 0.539 %.

Figure 4 shows the density variations of RP-3 versus temperature under different pressure conditions. Similar with other fluids,[2,3,9,10] the density of RP-3 increases as pressure increases and decreases as temperature increases. It is seen from Figure 4 that the density of RP-3 decreases dramatically when the temperature reaches to about 604.45 K at 2 MPa and 641.27 K at 2.34 MPa. The reason is: small scale bubbles generated at 604.45 K under 2 MPa pressure conditions because the temperature is close to its phase transient point of 601.3 K at 2 MPa; large density fluctuation occurs because the temperature 641.27 K at 2.34 MPa is close to the critical point (T_c = 645.04 K). As pressure increases, the trend of the density changing with temperature changes smoothly; the higher the pressure, the smoother the trend of the density changing. This phenomenon is accordant with ideal trend of the density of pure fluid at supercritical conditions.[14]

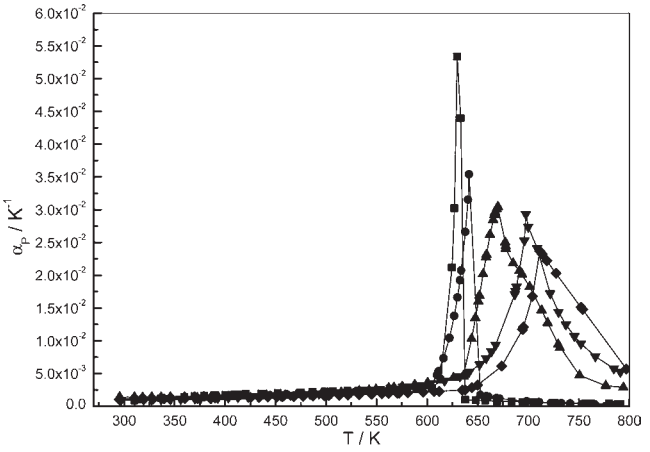

Figure 5. Effects of temperature and pressure on the isobaric thermal expansion of RP-3. ■, 2 MPa; ●, 2.24 MPa; ▲, 3 MPa; ▼, 4 MPa; ♦, 5 MPa.

3.3. Isobaric Thermal Expansion of RP-3. The fitted experimental density in this work can be used to derive the isobaric thermal expansion, α_P, which is defined as

$$\alpha_P = -\frac{1}{\rho}\left(\frac{\partial \rho}{\partial T}\right)_P \quad (9)$$

Figure 5 shows the isobaric thermal expansion of RP-3 versus temperature from sub- to supercritical pressure conditions. It is

dx.doi.org/10.1021/je200258g |J. Chem. Eng. Data 2011, 56, 2980–2986

seen from Figure 5 that for a fixed pressure: α_P increases with the increase of temperature when the temperature is lower than the phase transient point, critical point, or pseudocritical point; when the temperature is close to the phase transient point, the critical point, or the pseudocritical point, α_P increases rapidly and reaches to the peak value at these points due to the largest change of density; when the temperature is greater than the phase transient point, the critical point, or the pseudocritical point, α_P decreases with the increase of temperature. In addition, the temperature of the peak value of α_P increases with the increase of pressure, and the peak value of α_P decreases with the increase of pressure. In fact, the temperatures of the peak value of α_P at supercritical pressures are identified as the critical or the pseudocritical temperatures of RP-3. At (3, 4, and 5) MPa conditions, the pseudocritical temperatures of RP-3 are determined as (669.88, 698.59, and 710.71) K, respectively. But under critical pressure conditions, the temperature of the peak value of α_P is 641.27 K, which is a little different from the result (645.04 K) of visualization experiments. The reason is probably that the density of RP-3 fluctuated dramatically at the critical point which increased the measurement error.

4. CONCLUSION

A novel density measurement method is proposed based on the mass conservation equation for the density measurement of single phase flow including supercritical fluids at high pressure and temperature conditions. The density of a typical endothermic hydrocarbon fuel (RP-3, T_c = 644.5 K, P_c = 2.34 MPa) has been measured at the temperature range of (295 to 796) K and under pressures from (0.1 to 5) MPa.

The results of the densities of RP-3 are fitted as polynomials to analyze the AAD and the MAD: before the critical point, AAD = 0.264 % and MAD = 1.52 %, respectively; near the critical point, AAD = 1.05 % and MAD = 2.42 %, respectively; beyond the critical point, AAD = 0.833 % and MAD = 3.29 %, respectively; for all values, AAD = 0.539 %. In addition, the density of RP-3 at the critical point is identified as 221.18 $kg \cdot m^{-3}$ under the aforementioned compositions. Moreover, the isobaric thermal expansion α_P of RP-3 has been derived from the fitted experimental density data. The result shows that the peak value of α_P decreases with the increase of pressure, and the temperature of the peak value of α_P increases with the increase of pressure. In fact, the peak value of α_P can be used to determine the pseudocritical point of RP-3; at (3, 4, and 5) MPa they are identified as (669.88, 698.59, and 710.71) K, respectively.

AUTHOR INFORMATION

Corresponding Author

*E-mail: zhang_cb@sjp.buaa.edu.cn. Fax: +86-10-82314545.

Funding Sources

This work is funded by the Natural Science Foundation of China under Contract No. 50676005.

ACKNOWLEDGMENT

The authors would like to thank Guo-zhu Liu and Hai-wang Li for their technical support.

REFERENCES

(1) Huang, H.; Spadaccini, L. J.; Sobel, D. R. Fuel-cooled thermal management for advanced aeroengines. *J. Eng. Gas Turbines Power* **2004**, *126* (2), 284–293.

(2) Fedele, L.; Pernechele, F.; Bobbo, S.; Scattolini, M. Compressed Liquid Density Measurements for 1,1,1,2,3,3,3-Heptafluoropropane (R227ea). *J. Chem. Eng. Data* **2007**, *52* (5), 1955–1959.

(3) Lei, Y.; Chen, Z.; An, X.; Huang, M.; Shen, W. Measurements of Density and Heat Capacity for Binary Mixtures {x Benzonitrile + (1 − x) (Octane or Nonane)}. *J. Chem. Eng. Data* **2010**, *55* (10), 4154–4161.

(4) Fujiwara, K.; Nakamura, S.; Noguchi, M. Critical Parameters and Vapor Pressure Measurements for 1,1,1-Trifluoroethane (R-143a). *J. Chem. Eng. Data* **1998**, *43* (1), 55–59.

(5) Wilson, L. C.; Wilding, W. V.; Wilson, H. L.; Wilson, G. M. Critical Point Measurements by a New Flow Method and a Traditional Static Method. *J. Chem. Eng. Data* **1995**, *40* (4), 765–768.

(6) Rosenthal, D. J.; Gude, M. T.; Teja, A. S.; Mendez-Santiago, J. The critical properties of alkanoic acids using a low residence time flow method. *Fluid Phase Equilib.* **1997**, *135* (1), 89–95.

(7) Smith, R. L.; Teja, A. S.; Kay, W. B. Measurement of critical temperatures of thermally unstable n-Alkanes. *AIChE J.* **1987**, *33* (2), 232–238.

(8) Nikitin, E. D.; Pavlov, P. A.; Skripov, P. V. Measurement of the critical properties of thermally unstable substances and mixtures by the pulse-heating method. *J. Chem. Thermodyn.* **1993**, *25* (7), 869–880.

(9) Yun, S. L. J.; Dillow, A. K.; Eckert, C. A. Density Measurements of Binary Supercritical Fluid Ethane/Cosolvent Mixtures. *J. Chem. Eng. Data* **1996**, *41* (4), 791–793.

(10) Dai, H. J.; Simonson, J. M.; Cochran, H. D. Density Measurements of Styrene Solutions in Supercritical CO_2. *J. Chem. Eng. Data* **2001**, *46* (6), 1571–1573.

(11) Fandiño, O.; Comuñas, M. J. P.; Lugo, L.; López, E. R.; Fernández, J. Density Measurements under Pressure for Mixtures of Pentaerythritol Ester Lubricants. Analysis of a Density−Viscosity Relationship. *J. Chem. Eng. Data* **2007**, *52* (4), 1429–1436.

(12) Stringari, P.; Scalabrin, G.; Richon, D. Liquid Density Measurements for the Propylene + 2-Propanol + Water System. *J. Chem. Eng. Data* **2009**, *54* (8), 2285–2290.

(13) Wagner, W.; Pruss, A. The IAPWS formulation 1995 for the thermodynamic properties of ordinary water substance for general and scientific use. *J. Phys. Chem. Ref. Data* **2002**, *31* (2), 387–535.

(14) Krishnan, A.; Zhou, N.; Giridharan, M. G. Transport phenomena in supercritical fluids. In the *26th Fluid Dynamics Conference*, San Diego, CA, 1995.